Bi-Directional Multi-Hop Wireless Pipeline Using Physical-Layer Network Coding

Haoyuan Zhang, *Student Member, IEEE*, and Lin Cai, *Senior Member, IEEE*

***Abstract*— In this paper, the design of multi-hop physical layer network coding (PNC) is investigated. In the existing multi-hop PNC designs, the effects of error propagation and mutual-interference are not well addressed. Error propagation refers to that the estimation error at any node may propagate to the neighboring nodes, which may result in serious end-to-end bit errors. The impact of the mutual-interference from other transmitting nodes to a receiver determines the upper bound SINR of two neighboring nodes given end-to-end SNR. By carefully addressing these issues, we propose two multi-hop PNC designs, the direct multi-hop PNC (D-MPNC) and the stored multi-hop PNC (S-MPNC), where both designs achieve the throughput upper bound of one symbol per symbol duration, which is the same as that of the traditional PNC with a single relay. There is a tradeoff between the applications of D-MPNC and S-MPNC, which targets for simple-implementation and optimal end-to-end bit error rate (BER), respectively. We provide the detailed designs of D-MPNC and S-MPNC and obtain the end-to-end BER bounds theoretically. Extensive simulation results demonstrate the performance gain of the proposed multi-hop PNC compared with the traditional PNC in terms of end-to-end BER and end-to-end throughout.**

***Index Terms*— Physical layer network coding, multi-hop, error propagation.**

I. Introduction

In A two-way relay channel (TWRC) network, physical layer network coding (PNC) [1], [2] allows the concurrent transmissions from the sources to the relay in the multiple-access stage. The network-coded symbol, which is obtained from the superimposed signals and contains the data of two sources, is broadcast back to the sources in the broadcast stage. Bidirectional information exchange is achieved by letting any source extract the other source's information from the network-coded symbol with the knowledge of its own original data. PNC was heavily studied considering a single relay. An inspiring multi-hop PNC was proposed in [1]. However, the error propagation effect was not fully investigated, which may result in endless bit estimation errors. Also, the impact of the mutual-interference from other transmitting nodes is not well addressed in the existing multi-hop PNC designs [1], [3]–[8].

Manuscript received April 6, 2017; revised July 24, 2017; accepted September 8, 2017. Date of publication September 26, 2017; date of current version December 8, 2017. The associate editor coordinating the review of this paper and approving it for publication was W. H. Mow. *(Corresponding author: Lin Cai.)*

The authors are with the Department of Electrical and Computer Engineering, University of Victoria, Victoria, BC V8P 5C2, Canada (e-mail: hyuan@uvic.ca; cai@uvic.ca).

Color versions of one or more of the figures in this paper are available online at http://ieeexplore.ieee.org.

Digital Object Identifier 10.1109/TWC.2017.2755026

There are several major challenges to design and generalize multi-hop PNC. First, in the traditional PNC with a single relay, the transmission period is two slots and different periods are independent. In multi-hop PNC, one error at any of the relay may affect the correctness of the other nodes in several even all of the following slots. Second, the received information in the previous slots can be positively applied by the sources and the relays [1] in multi-hop PNC. The difficulty is that the number of options to apply these information at any node goes up exponentially with the increase of the transmission slots, and improperly applying these information may degrade the performance. Third, different from the single relay case, a receiver in multi-hop PNC may not only receive the useful information from the neighbouring nodes, but also the non-negligible interference from other transmitting nodes depending on the scheduling. Generally speaking, the design and generalization of multi-hop PNC transmission protocol should jointly consider the impact of the error propagation, the combination of information in multiple slots, and the mutual-interference to maximize the end-to-end throughput and minimize the BER.

The main contributions of this paper are three-fold. First, we investigate the key issues in multi-hop PNC design, including the impact of the error propagation and the mutual-interference from other transmitting nodes, and provide guidelines of how to properly utilize the previously received information at any node. Second, by carefully addressing the key issues, we propose two multi-hop PNC designs, the direct multi-hop PNC (D-MPNC) and the stored multi-hop PNC (S-MPNC). D-MPNC is simple to implement while S-MPNC outperforms D-MPNC in terms of end-to-end BER. The throughput upper bound of both D-MPNC and S-MPNC is one symbol per symbol duration, the same as that of the case with a single relay. Third, we obtained the end-to-end BER bounds of D-MPNC and S-MPNC theoretically. In addition, we evaluate the end-to-end BER and throughput performance of the proposed multi-hop PNC designs under various channel settings. The impact of relays' locations is further studied.

The rest of this paper is organized as follows. Related work are summarized in Sec. II. Sec. III introduces the system model and the key issues in multi-hop PNC design. In Sec. IV and Sec. V, we elaborate the designs and analysis of D-MPNC and S-MPNC, respectively. Simulation results are presented in Sec. VI, and the concluding remarks are presented in Sec. VII.

II. Related Work

Traditional PNC has been extensively studied from theory [9]–[16] to implementation [17]. The PNC design was

generalized with a star topology in [18], where the information exchange of four nodes with the help of one relay was considered. He and Liew [19] further generalized the star-topology design with an arbitrary number of sources. Lin et al. [20] studied the throughput performance of several network coding (NC) schemes using the slotted ALOHA protocol and proposed a hybrid NC scheme, where two user groups exchange information aided by one relay node. The throughput capacity of PNC in a distributed wireless network coordinated with IEEE 802.11 distributed coordination function (DCF) was investigated, with the scenarios of multiple user-pairs and one relay in [21], and Canonical network in [22], respectively.

The design of multi-hop PNC has received less attention due to its inherent difficulty. Wang *et al.* [7] proposed a directional multi-hop PNC design. Popovski and Yomo [3] provided the specific PNC designs with a given number of relays. The design of multi-hop analog network coding (ANC) in a linear topology was generalized with the outage probability analysis in [4]–[6]. The design in [4] can outperform the non-PNC scheme with a small number of the relays, while the design in [5] can outperform the non-PNC scheme with a large number of nodes. Wang et al. [6] further extended [4] and [5], and its end-to-end throughput upper bound decreases with the increase of the number of relays. An inspiring generalization of multi-hop PNC was proposed in [1], which achieves the end-to-end throughput upper bound of one symbol per symbol duration. However, the error propagation effect is not addressed, which may result in serious bit errors as discussed in Sec. III-C. Wang et al. [8] studied multi-hop PNC design with full-duplex nodes, while how to synchronize the signals from neighboring nodes and the self-interference signal, and the error propagation problem remain open issues. Also the mutual-interference from other transmitting nodes are not addressed in the existing multi-hop PNC and ANC designs.

In this paper, the impact of the error propagation and the mutual-interference from other transmitting nodes in multi-hop PNC is addressed. We propose two multi-hop PNC designs targeting on the simple-implementation and the optimal end-to-end BER, respectively. The tradeoff between these two designs are discussed in Sec. V-D. Both designs can achieve the maximum end-to-end throughput upper bound of one symbol per symbol duration, the same as the case with a single relay.

III. Design Criterion of Multi-Hop PNC

A. System Model

Consider a multi-hop TWRC network as shown in Fig. 1, where sources A and B want to exchange information with the help of multiple relays arranged in a linear topology. The number of relays is denoted by N. In this paper, each node uses the BPSK modulation. Each node is equipped with one antenna and works in a half-duplex mode. We assume symbol-level synchronization at the relays and perfect channel estimations at the receivers, which have been shown feasible in [11], [17], and [23]. The carrier frequency synchronization is not assumed, which is much harder to achieve in a practical system due to the frequency mismatch at the transmitter's and the receiver's oscillator. Thus, a relative phase offset for the two superimposed signals is considered.

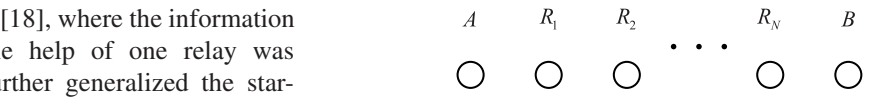

Fig. 1. System model.

To apply PNC, all the nodes, including the sources and the relays, follow a transmitting-and-receiving pattern with one-slot interval, and the transmitters and the receivers are separated apart from each other. In order to achieve the end-to-end throughput of one symbol per symbol duration, i.e., the same as that of the traditional PNC with a single relay, there cannot exist any idle slot except the constant initialization slots.[1] We consider that the slot duration is large enough for a packet transmission and each transmitting node transmits one packet per slot. Depending on how many useful signals are received at the receiver, the transmissions of multi-hop PNC can be divided into two categories, the multiple-access transmission and the single-hop transmission. The multiple-access transmission refers to that in each symbol duration, two useful signals transmitted from the neighbouring nodes are superimposed at a relay, and the single-hop transmission refers to that a relay transmits signals to a destination. Note that in multi-hop PNC, all the nodes not only receive the useful signals, but also the mutual-interference from the other transmitting nodes, which will be explained in Sec. III-D and considered in Sec. IV and Sec. V.

B. Procedure of the Proposed Multi-Hop PNC

Denote the total number of relays by N. Denote the indexes of the time-slot and the relay as i and j, respectively, where i is a positive integer and $j \in \{1, 2, \cdots, N\}$. For the multiple-access transmission, the received symbol of the j-th relay at the i-th slot is

$$Y_{r_{j,i}} = H_{r_{j-1,i}}(1 - 2S_{r_{j-1,i}}) + H_{r_{j+1,i}}(1 - 2S_{r_{j+1,i}}) + I + N_j, \tag{1}$$

where $H_{r_{j-1,i}}$ and $H_{r_{j+1,i}}$ are the channel gains over the links between the $(j-1)$-th node and the j-th relay, and that between the j-th relay and the $(j+1)$-th node, respectively. N_j is the additive Gaussian noise with a variance of σ^2 and I is the interference power of the other interfering signals. $S_{r_{j-1,i}}$ and $S_{r_{j+1,i}} \in \{0, 1\}$ are the binary data from the $(j-1)$-th node and the $(j+1)$-th node,[2] respectively. The network-coded symbol obtained by the j-th relay is

$$S_{r\_xor_{j,i}} \hat{S}_{r_{j-1,i}} \oplus \hat{S}_{r_{j+1,i}}, \tag{2}$$

where $\hat{S}_{r_{j-1,i}}$ and $\hat{S}_{r_{j+1,i}}$ are the estimation results of the superimposed symbols from the neighbouring relays,[3] which

[1] When the number of the transmission slots goes to infinity, the impact of the constant number of initialization slots to the end-to-end throughput can be neglected.

[2] For BPSK, the binary data $S_{data} = 0$ and 1 will be modulated to the transmitted symbols $S_{symbol} = 1$ and -1, respectively, i.e., $S_{symbol} = 1 - 2S_{data}$ in (1).

[3] Note that the estimations of $\hat{S}_{r_{j-1,i}}$ and $\hat{S}_{r_{j+1,i}}$ are intermediate steps. The final information that the relay applies is the network-coded symbol.

can be obtained by

$$(\hat{S}_{r_{j-1,i}}, \hat{S}_{r_{j+1,i}}) = \underset{s_{r_{j-1,i}}, s_{r_{j+1,i}} \in \{0,1\}}{\operatorname{argmin}} |Y_{r_{j,i}} - H_{r_{j-1,i}}(1 - 2s_{r_{j-1,i}}) - H_{r_{j+1,i}}(1 - 2s_{r_{j+1,i}})|^2. \tag{3}$$

Note that for the j-th relay, it may not directly transmit the network-coded symbol $S_{r\_xor_{j,i}}$ in (2) in the following slot, as the received information in the previous slots may be positively applied and combined with $S_{r\_xor_{j,i}}$. Similarly, the sources may not simply transmit X_t and Y_t at the transmitting slots, where t is the index of the source data, as the received information in the previous slots can be positively applied. We will explain these issues in Sec. III-C by an example, and in Sec. IV and Sec. V in detail.

For the single-hop transmission from the sources' neighbouring relays to the sources, at the i-th slot, $i \in \{2, 4, \cdots\}$, the received signal at source A from the first relay is

$$Y_{a_i} = H_{a_i}(1 - 2S_{r_{1,i}}) + N_a, \tag{4}$$

where H_{a_i} is the channel gain over the link between source A and the first relay, and N_a is the summation of the Gaussian noise and the mutual-interference from all other transmitting nodes. The estimation of $S_{r_{1,i}}$ can be obtained by

$$\hat{S}_{r_{1,i}} = \underset{s_{r_{1,i}} \in \{0,1\}}{\operatorname{argmin}} |Y_{a_i} - H_{a_i}(1 - 2s_{r_{1,i}})|^2. \tag{5}$$

The detection at source B can be similarly obtained as (4) and (5). Note that different from the traditional PNC with a single relay, in multi-hop PNC, source A may not directly obtain the target information from $\hat{S}_{r_{1,i}}$, as $\hat{S}_{r_{1,i}}$ may be an XOR result of multiple symbols. How to obtain the target information from $\hat{S}_{r_{1,i}}$ will be explained in Sec. III-C by an example and explained in Sec. IV-B, and Sec. V-B in detail.

The transmission protocol design of multi-hop PNC is challenging. How to positively apply the received information in the previous slots at all the nodes is a tricky issue, and improperly applying the previously received information may result in serious error propagation in Sec. III-C. Also, different strategies of applying these information will result in different symbol combination patterns at the relays, which further challenges the sources how to identify the received symbol combinations varied in different slots and how to extract the target information from the symbol combinations by a generalized decoding algorithm.

C. Error Propagation in Multi-Hop PNC

Error propagation is an important issue in the multi-hop PNC design and improper design may result in serious error propagation. We use the multi-hop PNC with three relays in [1] as shown in Fig. 2 to explain the error propagation impact.

By the scheduling introduced in [1], in the i-th slot, $i \in \{5, 7, \cdots\}$, the source A (B) transmits the XOR result of $X_{\frac{i+1}{2}}$ ($Y_{\frac{i+1}{2}}$) and the estimated $\hat{Y}_{\frac{i-3}{2}}$ ($\hat{X}_{\frac{i-3}{2}}$) in the last slot. For example, in the fifth slot, source A transmits the XOR result of

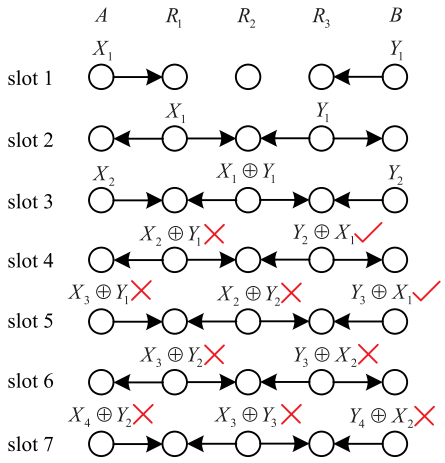

Fig. 2. Impact of the error propagation in multi-hop PNC.

X_3 and $\hat{Y}_1$ obtained in the fourth slot. The relays transmit the XOR results of the two network-coded symbols obtained in the last slot and the last three slots. For example, in the fifth slot, the second relay transmits $X_2 \oplus Y_2$, which is the XOR result of the network-coded symbol $X_2 \oplus Y_1 \oplus Y_2 \oplus X_1$ obtained in the fourth slot and that $X_1 \oplus Y_1$ obtained in the second slot.

We will show that the above scheduling may result in infinity end-to-end estimation errors. In Fig. 2, consider the case that if and only if the estimation result of $X_2 \oplus Y_1$ is erroneous at the first relay in the third slot. The transmitted symbol from the first relay in the fourth slot, i.e., $X_2 \oplus Y_1$, is erroneous accordingly. The impact on the following slots are marked by correctness marks, which specify the correctness of the received network-coded symbols at different relays in the following slots. Note that, although in the fifth slot the binary results of $X_3 \oplus Y_1$ and $X_2 \oplus Y_2$ are both erroneous at the first relay and the second relay, respectively, the resulting network-coded symbol $X_3 \oplus Y_2$ at the second relay in the sixth slot is still erroneous by XOR the previous erroneous network-coded symbol $X_2 \oplus Y_1$. We can easily find that all the end-to-end estimations of Y_i, $i \in \{1, 2, \cdots\}$ and X_i, $i \in \{2, 3, \cdots\}$ at the sources are erroneous. Thus, improperly utilizing the received information in the previous slots can result in serious end-to-end bit errors. How to control and minimize the error propagation is an important issue in multi-hop PNC, which directly determines the end-to-end throughput.

Note that we can avoid infinite error propagation using end-to-end error detection and packet retransmission at the cost of a lower throughput. For example, in order to remove the erroneous $X_2 \oplus Y_1$ in Fig. 2, all the packets from slot 3 to slot 6 should be discarded in order to remove the error information in the multi-hop PNC pipeline.

D. Mutual-Interference in Multi-Hop PNC

Different from the traditional PNC with a single relay, in multi-hop, the received signals at any node not only contain the useful information from the neighbouring nodes, but also the possible mutual-interference from all other transmitting nodes depending on the scheduling [24], [25]. For example, consider the multi-hop PNC with three relays

as shown in Fig. 2. When the first relay is receiving two useful signals from source A and the second relay, it also suffers from the mutual-interference from source B. Similar mutual-interferences exist for source A, the third relay and source B coming from the third relay, source A and the first relay, respectively. With the increase of the relay number, one receiver may suffer from the mutual-interference from more than one node.

In this paper, for fair comparison, the total transmission power at all the nodes in any two continuous slots are fixed and denoted as $2E_b$. The distance between sources A and B is d (m) and the path-loss exponent is α. The end-to-end SNR (dB), i.e., SNR_{ab}, is defined as the single-hop SNR considering the direct transmission without PNC, which can be expressed as

$$\mathrm{SNR}_{ab}(\mathrm{dB}) = 10\log_{10}(\frac{E_b d^{-\alpha}}{2\sigma^2}), \tag{6}$$

where $\mathrm{SNR}_{ab}(\mathrm{dB})$ denotes the direct transmission from the two sources without PNC with transmission power E_b. For the multi-hop PNC with N relays, the transmission power for each node is $\frac{2E_b}{N+2}$, and the hop-distance between any two nodes is $\frac{d}{N+1}$ equally.[4] Different from the traditional PNC, in multi-hop PNC, due to the mutual-interference, SINR should be considered for any node instead of SNR. The SINR(dB) for the k-th node, $k \in \{1, 2, \cdots, N+2\}$ is in (7), where $\sum_{i=1}^{0}(\cdot) = 0$, $\sum_{i=1}^{\lfloor\frac{k-1}{3}\rfloor} \frac{2E_b}{N+2}(\frac{(2i+1)d}{N+1})^{-\alpha}$ and $\sum_{j=1}^{\lfloor\frac{N+2-k}{3}\rfloor} \frac{2E_b}{N+2}(\frac{(2j+1)d}{N+1})^{-\alpha}$ are the power of the interference from the nodes on the left-side and the right-side of the k-th node, respectively. From (6) and (7), shown at the bottom of this page, when the end-to-end SNR_{ab} (dB) is sufficiently large, it is easy to find that $\mathrm{SINR}_k(\mathrm{dB})$ will be upper bounded by $10\alpha\log_{10}(3)$, where α is the path-loss exponent and 3 is determined by the distance ratio of the closest interference node, i.e., 3 hop-distance away, and the neighbouring node. The brief explanation is as follows in (8). When $\mathrm{SNR}_{ab}(\mathrm{dB}) = 10\log_{10}(\frac{E_b d^{-\alpha}}{2\sigma^2})$ is large enough, i.e., $d^{-\alpha} \gg 2\sigma^2/E_b$, we have (8) shown at the bottom of this page.

[4]We also studied the impact when the relays are not equally located in Sec. VI-C.

E. Proposed Multi-Hop PNC Designs

In this paper, depending on the operations of the sources and the relays, we propose two multi-hop PNC designs, D-MPNC and S-MPNC, and the error propagation and mutual-interference issues are well addressed in both designs. In D-MPNC, the operations of the relays are the same as that in the traditional PNC with a single relay, i.e., to demodulate the superimposed symbols from the neighbouring nodes and directly broadcast the network-coded symbol constructed from the demodulation results. In other words, the previous received information are not utilized by the relays in D-MPNC. In S-MPNC, we target to obtain and generalize the optimal multi-hop PNC design in terms of minimizing end-to-end BER. All of the sources and the relays are able to apply the previously received information in S-MPNC. The key issues in the design of D-MPNC include how the sources identify the received symbol combination from the neighbouring relays and how to design the generalized decoding algorithm for the sources as the received symbol combination varies in different slots. The key issues in the design of S-MPNC include how to properly apply the previously received information to minimize the error propagation impact, how to design the generalized decoding algorithm at the sources, how to minimize the end-to-end BER and maximize the end-to-end throughput and how to generalize S-MPNC with an arbitrary number of relays. We present the designs of D-MPNC and S-MPNC in Sec. IV and Sec. V, respectively.

$$\mathrm{SINR}_k(\mathrm{dB}) = 10\log_{10}\frac{\frac{2E_b}{N+2}(\frac{d}{N+1})^{-\alpha}}{2\sigma^2 + \sum_{i=1}^{\lfloor\frac{k-1}{3}\rfloor}\frac{2E_b}{N+2}(\frac{(2i+1)d}{N+1})^{-\alpha} + \sum_{j=1}^{\lfloor\frac{N+2-k}{3}\rfloor}\frac{2E_b}{N+2}(\frac{(2j+1)d}{N+1})^{-\alpha}}. \tag{7}$$

$$\begin{aligned}
\mathrm{SINR}_k(\mathrm{dB}) &= 10\log_{10}\frac{\frac{2E_b}{N+2}(\frac{d}{N+1})^{-\alpha}}{2\sigma^2 + \sum_{i=1}^{\lfloor\frac{k-1}{3}\rfloor}\frac{2E_b}{N+2}(\frac{(2i+1)d}{N+1})^{-\alpha} + \sum_{j=1}^{\lfloor\frac{N+2-k}{3}\rfloor}\frac{2E_b}{N+2}(\frac{(2j+1)d}{N+1})^{-\alpha}} \\
&= 10\log_{10}\frac{d^{-\alpha}}{2\sigma^2\frac{(N+1)^{-\alpha}(N+2)}{2E_b} + \sum_{i=1}^{\lfloor\frac{k-1}{3}\rfloor}((2i+1)d)^{-\alpha} + \sum_{j=1}^{\lfloor\frac{N+2-k}{3}\rfloor}((2j+1)d)^{-\alpha}} \\
&< 10\log_{10}\frac{d^{-\alpha}}{\sum_{i=1}^{\lfloor\frac{k-1}{3}\rfloor}((2i+1)d)^{-\alpha} + \sum_{j=1}^{\lfloor\frac{N+2-k}{3}\rfloor}((2j+1)d)^{-\alpha}} \\
&< 10\log_{10}\frac{d^{-\alpha}}{(3d)^{-\alpha}} = 10\alpha\log_{10}3.
\end{aligned} \tag{8}$$

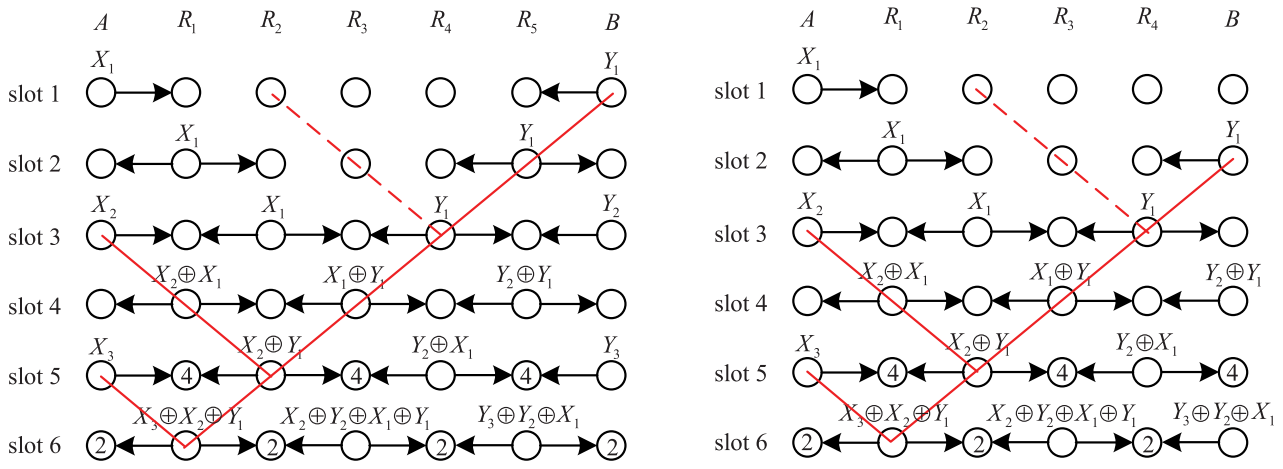

(a) D-MPNC with $N = 5$. (b) D-MPNC with $N = 4$.

Fig. 3. Transmission graph of D-MPNC.

IV. Design of D-MPNC

In this section, we provide the design of D-MPNC. D-MPNC benefits from the simple implementation, as the functions of the relays are the same as that of the traditional PNC with a single relay, i.e., to receive the superimposing signals and broadcast the network-coded symbol directly. We illustrate the design of D-MPNC and obtain the bound of end-to-end BER for D-MPNC.

A. Procedure of D-MPNC

The procedure of D-MPNC with odd number relays can be summarized as follows:

1) The sources and the even-indexed relays transmit in the odd slots and receive in the even slots. The odd-indexed relays transmit in the even slots and received in the odd slots.

2) Source A and B transmit $X_{\frac{i+1}{2}}$ and $Y_{\frac{i+1}{2}}$, respectively, in an odd slot.[5]

3) All the relays directly transmit the network-coded symbol obtained in (2), which is the same as that of the traditional PNC with a single relay.

The D-MPNC with an even-number of N relays can be extrapolated from the D-MPNC with $N+1$ relays by letting source B transmit the XOR result of $Y_{\frac{i}{2}}$, $i \in \{2, 4, \cdots\}$ and the last received binary information. We use Figs. 3(a) and 3(b) as two examples to explain the procedure of D-MPNC, which show the transmission graph of D-MPNC with $N = 5$ and $N = 4$, respectively. In Fig. 3(a), the first four slots are the initializing slots, as the first two target information X_1 and Y_1 have not been delivered to the other source. From the fifth slot, two sources can exchange two packets end-to-end by every two slots. Thus, when the number of the transmission slots is sufficiently large, the end-to-end throughput upper bound is one symbol per symbol duration as two packets are delivered in any two slots. In Fig. 3(b), it shows that D-MPNC with $N = 4$ can be extrapolated from D-MPNC with $N = 5$ by letting source B transmit the XOR result of $Y_{\frac{i}{2}}$, $i \in \{2, 4, \cdots\}$ and the last received binary information. For example, in the 4-th slot, source B transmits $Y_2 \oplus Y_1$.

From Fig. 3, we can see that with the increase of the transmission slots, the transmitting symbol at the relay may be an XOR result of a symbol combination containing more and more symbols. However, it is unnecessary for the relay to identify any bit in the symbol combination. From the relay's perspective, it simply receives two superimposed signals from the neighbouring nodes and broadcasts the network-coded symbol obtained by (2) without knowing the details of the symbol combination. Note that the challenge part is that it is necessary for the sources to identify the symbol combination from the neighbouring relays in (5) and then extract the target information from the other source, which will be introduced in the next subsection.

B. Design of the Decoding Algorithm for D-MPNC

The generalized decoding algorithm for D-MPNC is presented in this subsection, which specifies the iterative algorithm for the sources to extract the target information of the other source from the obtained symbol combinations. The detection algorithm design for D-MPNC includes two steps, 1) bit combination pattern identification and 2) iterative detection algorithm design. Step 1) is to identify the received symbol combination from the neighbouring relay, which varies in different slots. Step 2) is to extract the target information from the identified symbol combination. Note that step 1) is done offline, while step 2) is the online detection algorithm. Step 1) is to prepare for the design of step 2), the online iterative detection algorithm.

We use D-MPNC with $N=5$ in Fig. 3(a) as an example to illustrate the design criterion, followed by D-MPNC designs with other numbers of relays.

1) Identifying the Received Symbol Combination: In the i-slot, $i \in \{2, 4, \cdots\}$, for source A, the target estimating symbol from source B is $Y_{\frac{i-N+1}{2}}$, due to that symbol $Y_{\frac{i-N+1}{2}}$

[5]For notation simplicity, we assume that one symbol X_i (Y_i) is transmitted in each slot where the slot duration equals the symbol duration, and the design and analysis can be applied to the general cases that a fixed number of symbols are transmitted per slot where the slot duration equals the transmission time of these symbols.

takes $N+1$ slots to be delivered from source B to source A. The precondition for source A to extract the target information $Y_{\frac{i-N+1}{2}}$ is to identify the symbol combination of $S_{r_{1,i}}$ in (5). For D-MPNC, the sources can identify the received symbol combination of $S_{r_{1,i}}$ according to a graph-based algorithm. Considering D-MPNC with $N=5$ as shown in Fig. 3(a), the graph-based algorithm is described as follows:

1) Generate a tree with the root of relay R_1 in the i-th slot, $i \in \{6, 8, \cdots\}$.

2) Visit the two neighbouring nodes of all the roots in the $(i-1)$-th slot. If any node is not a source node nor it is visited twice, update it as a new root.

3) Generate edges connecting root R_1 in the i-th slot with the new root and the visited source in the $(i-1)$-th slot.

4) Repeat steps 2) and 3) until the first slot is considered.

5) The received symbol combination at source A in the i-th slot, i.e., $S_{r_{1,i}}$, is the XOR combination result of all the symbols at the source nodes visited.

We provide an example to explain the above graph-based algorithm. In Fig. 3(a), the received symbol combination at source A in the sixth slot can be obtained by selecting the relay R_1 in the sixth slot as the root in step 1). In step 2), visit source A and relay R_2 in the fifth slot. Update R_2 as a new root as it is only visited once. In step 3), generate two edges connecting root R_1 in the sixth slot with source A and R_2 in the fifth slot, respectively. In step 4), steps 2) and 3) are repeated until the first slot is visited. In step 5), the symbol combination of $S_{r_{1,6}}$ in the sixth slot can be expressed by taking the XOR of all the symbols at the source nodes visited, i.e., $S_{r_{1,6}} = X_3 \oplus X_2 \oplus Y_1$. By observing the tree generated in the graph presented in the red edges, we can easily find that the received symbol combination $S_{r_{1,i}}$ at source A follows a pattern of $X_i \oplus X_{i-1} \oplus Y_{i-2} \oplus X_{i-3} \oplus Y_{i-4} \cdots$ until the index is 1.

2) Generalizing the Iterative Decoding Algorithm: The graph-based algorithm identifies the received symbol combination at the sources from the neighbouring relays. We target on generalizing the decoding algorithm for D-MPNC by the help of the pattern obtained from the graph-based algorithm. We use D-MPNC with $N=5$ as an example, where source A (B) can extract the target information from the received symbol combination by an iterative decoding algorithm summarized as follows:

1) Maintain two buffers denoted as B_1 and B_2, which are initialized to be $B_1=0$ and $B_2=X_1$ at source A (B).

2) In the i-th slot, $i \in \{6, 10, 14, \cdots\}$,[6] obtain $\hat{S}_{r_{1,i}}$ by (5). Extract $\hat{Y}_j = \hat{S}_{r_{1,i}} \oplus X_{j+2} \oplus X_{j+1} \oplus B_1$, $j = \frac{i}{2}-2$. Update $B_1 = X_{j+2} \oplus \hat{S}_{r_{1,i}}$.

3) In the i-slot, $i \in \{8, 12, 16, \cdots\}$, obtain $\hat{S}_{r_{1,i}}$ by (5). Extract $\hat{Y}_j = \hat{S}_{r_{1,i}} \oplus X_{j+2} \oplus X_{j+1} \oplus B_2$, $j = \frac{i}{2}-2$. Update $B_2 = X_{j+2} \oplus \hat{S}_{r_{1,i}}$.

For example, in the sixth slot, $\hat{Y}_1$ can be obtained by $\hat{Y}_1 = \hat{S}_{r_{1,6}} \oplus X_3 \oplus X_2 \oplus B_1$, where $\hat{S}_{r_{1,6}} = X_3 \oplus X_2 \oplus \hat{Y}_1$ and $B_1=0$ by step 1), and then B_1 is updated to be $X_2 \oplus \hat{Y}_1$. In the tenth slot, $\hat{Y}_3$ can be obtained by $\hat{Y}_3 = \hat{S}_{r_{1,10}} \oplus X_5 \oplus X_4 \oplus B_1$, where $\hat{S}_{r_{1,10}} = X_5 \oplus X_4 \oplus \hat{Y}_3 \oplus X_2 \oplus \hat{Y}_1$, and then B_1 is updated to be $X_4 \oplus \hat{Y}_3 \oplus X_2 \oplus \hat{Y}_1$. Note that by the above iterative decoding algorithm, although $S_{r_{1,i}}$, B_1 and B_2 are the XOR combination of multiple symbols, the sources only need to maintain two binary results in buffers B_1 and B_2 without the requirement of identifying any of the individual symbol in the symbol combinations. Thus, the computation at the sources will not increase over time.

[6]The 6-th slot is the first slot that the target information Y_1 is delivered from source B to source A.

C. Decoding Algorithm of D-MPNC With Other Numbers of Relays

When $N=1$, D-MPNC deteriorates to the traditional PNC with single relay. The traditional PNC decoding algorithm can be directly applied.

When $N=3$, the received symbol pattern can be obtained according to the graph-based algorithm described in Sec. IV-B.1, i.e., in the i-th slot, $i \in \{4, 6, \cdots\}$, the received symbol combination at source A is $X_{\frac{i}{2}} \oplus X_{\frac{i}{2}-1} \oplus \hat{Y}_{\frac{i}{2}-1}$. Thus, the iterative decoding algorithm applied at source A is to extract $\hat{Y}_{\frac{i}{2}-1} = \hat{S}_{r_{1,i}} \oplus B$ by maintaining one buffer initialized with $B = X_2 \oplus X_1$ and updating by $B = X_{\frac{i}{2}} \oplus X_{\frac{i}{2}-1}$.

When $N=7$, according to the graph-based algorithm, in the i-th slot, $i \in \{8, 10, \cdots\}$, the received symbol combination at source A is $X_{\frac{i}{2}} \oplus X_{\frac{i}{2}-1} \oplus X_{\frac{i}{2}} \oplus \hat{Y}_{\frac{i}{2}-1}$. Thus, the iterative decoding algorithm applied at the source A is to extract $\hat{Y}_{\frac{i}{2}-3} = \hat{S}_{r_{1,i}} \oplus B$ by maintaining one buffer initialized with $B = X_4 \oplus X_3 \oplus X_1$ and updating by $B = X_{\frac{i}{2}} \oplus X_{\frac{i}{2}-1} \oplus X_{\frac{i}{2}-3}$.

The design of D-MPNC with an even number (N) of relays can be extrapolated from D-MPNC with $N+1$ relays. To generalize D-MPNC with an arbitrary number of N is challenging, because the transmission patterns of D-MPNC with different N are dynamic. For the D-MPNC with $N>7$, we can first design the case when N is an odd number and then obtain D-MPNC with $(N-1)$ by extrapolating from D-MPNC with N. To design the iterative algorithm for D-MPNC given N, we first need to identify the received symbol combination at the sources according to the graph-based algorithm described in Sec. B1, and then generalize the pattern of the received symbol combination, followed by designing the iterative decoding algorithm with the help of the symbol combination pattern. Note that for D-MPNC, to obtain a general decoding algorithm with an arbitrary number of relays is hard. Because the design purpose of D-MPNC is to simplify the relay operations, and thus the patterns of the received symbol combinations at the sources cannot be controlled, and the pattern may not have a good feature to be generalized.

D. End-to-End BER Analysis of D-MPNC

One of the main concern for multi-hop PNC design is the error propagation issue. In this section, we analyze the end-to-end BER performance of MPNC, which is defined as

$$P_{e2e} = (P\{\hat{X} \neq X\} + P\{\hat{Y} \neq Y\})/2. \quad (9)$$

For the multi-hop path with N relays, the per-hop distance is assumed the same. The transmission procedure of MPNC includes the multi-access and the single-hop transmissions,

which should be studied separately. We first obtain the relay mapping error rate (P_{xor}) of the multi-access transmission and the single-hop transmission error rates ($P_{a,r}$ and $P_{b,r}$) for the traditional PNC with a single relay, and then study the end-to-end BER for PNC with multiple relays.

1) Traditional PNC With a Single Relay: We first provide the estimations for the end-to-end error performance of the traditional PNC with a single relay. Note that the exact BER analysis of traditional PNC with a single relay has been given in [26]. Denote the channel gain over source-relay link between source A and the relay and that between source B and the relay as H_a and H_b, respectively, where H_a and H_b are complex numbers. According to [26] and [27], for the AWGN channel, the error performance of the multiple-access transmission can be estimated by

$$P_{xor} = 2P_{\theta\in(0,\frac{\pi}{2})} + 2P_{\theta\in(\frac{\pi}{2},\pi)}, \tag{10}$$

where $P_{\theta\in\{0,\frac{\pi}{2}\}} = P_{\theta\in\{\frac{3\pi}{2},2\pi\}}$ and $P_{\theta\in\{\frac{\pi}{2},\pi\}} = P_{\theta\in\{\pi,\frac{3\pi}{2}\}}$ due to the symmetry of the received constellation map at the relay. Define the amplitude ratio and the phase shift difference between H_a and H_b as γ and θ, respectively, where $H_a = H_b\gamma\exp(j\theta)$. Define function

$$G(\phi, L) = \frac{1}{2\pi}\int_0^{\phi}\exp(-\frac{L^2}{2\sigma^2\sin^2(\theta')})\mathrm{d}\theta', \tag{11}$$

we have

$$P_{\theta\in(0,\frac{\pi}{2})} = \frac{\frac{\pi}{2}-0}{2\pi}\frac{1}{2\pi}\int_0^{\frac{\pi}{2}}\{G(\frac{\pi}{2}+\tan^{-1}(\frac{1-\gamma\cos(\theta)}{\gamma\sin(\theta)}), H_b^2) + G(\frac{\pi}{2}+\tan^{-1}(\frac{\gamma-\cos(\theta)}{\sin(\theta)}), H_a^2)\}\mathrm{d}\theta, \tag{12}$$

$$P_{\theta\in(\frac{\pi}{2},\pi)} \approx \frac{\pi-\frac{\pi}{2}}{2\pi}G(\pi, H_b^2) + \frac{\pi-\frac{\pi}{2}}{2\pi}G(\pi, H_a^2). \tag{13}$$

Note that (12) is valid for the case of $\gamma \le 1$. When $\gamma > 1$, we need to swap H_a and H_b in (12). The error performance of the multiple-access transmission P_{xor} can be obtained by substituting (12) and (13) into (10).

The BER of the single-hop transmission $P_{i,r}$ over the link between source $i\in\{a,b\}$ and the relay can be obtained by

$$P_{i,r} = \frac{1}{2\pi}\int_0^{\pi}\exp(\frac{H_i^2}{2\sigma^2\sin^2(\theta')})\mathrm{d}\theta', \tag{14}$$

where $i\in\{a,b\}$. Thus, the end-to-end BER performance can be obtained by

$$P_{e2e} = \frac{P_{xor}(2-P_{a,r}-P_{b,r})+(1-P_{xor})(P_{a,r}+P_{b,r})}{2}. \tag{15}$$

The theoretical estimation and the simulation results comparison is shown in Fig. 4, we can see that (10) and (15) match the simulation results well.

2) End-to-End BER Bound of D-MPNC: We first study the error propagation impact in D-MPNC. We will show that the error propagation caused by single estimation error at the relay can be bounded by constant bits, and the end-to-end BER can be bounded by the sum of the individual effect of the multi-access and single-hop transmission errors. We use the case of D-MPNC with $N=5$ as shown in Fig. 5 to explain.

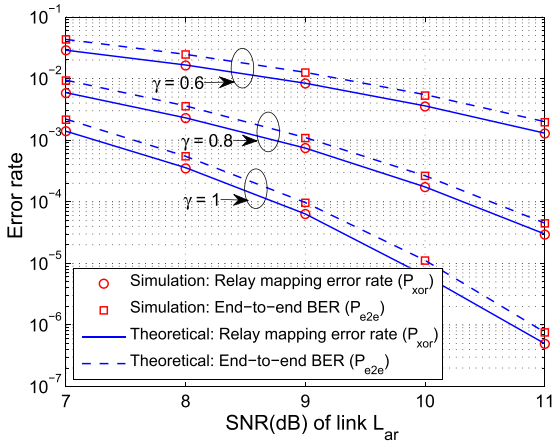

Fig. 4. Theoretical vs simulation.

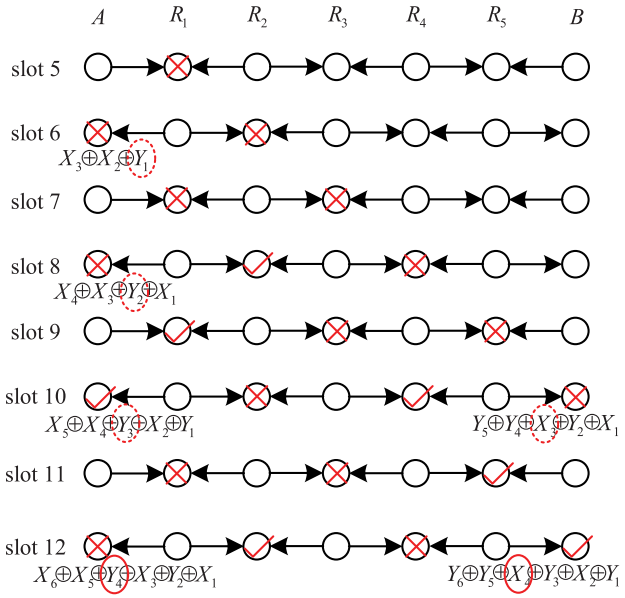

Fig. 5. Bounded error propagation in D-MPNC.

Consider the case that if and only if the superimposed symbol at R_1 in the fifth slot is in error as shown in Fig. 5. The received symbol combinations at A in the sixth and eighth slots are in error, which result in the erroneous estimations of Y_1 and Y_2, respectively. Similarly, the estimation of X_3 in the tenth slot at B is erroneous. Note that in the seventh slot, the superimposed symbol at R_1 is erroneous, as it is superimposed by the correct symbol from A and the erroneous symbol from R_2. In the tenth slot at A, although the received symbol combination, i.e., $X_5\oplus X_4\oplus Y_3\oplus X_2\oplus Y_1$, is correct, the estimation of Y_3 is still erroneous as the previous estimation of Y_1 is erroneous. After the tenth slot, all the estimations of the following bits are correct at both A and B. In other words, the error propagation effects are bounded by four bits in error, i.e., Y_1, Y_2, Y_3, X_3, which is briefly proved below.

From Fig. 5, we observe that the pattern from slot 12 to slot 15 is the same as that from slot 8 to slot 11, and repeats in a four-slot period. We first consider the bits received by source A. In the i-th slot, $i\in\{12,16,\cdots\}$, the received symbol combination by A, $X_{\frac{i}{2}}\oplus X_{\frac{i}{2}-1}\oplus Y_{\frac{i}{2}-2}\cdots Y_2\oplus X_1$,

TABLE I
LOWER BOUND END-TO-END BER OF D-MPNC

N	End-to-end BER bound
$N=2$	$\frac{3}{2}\mathrm{P}_{xor\_R_1}+\mathrm{P}_{xor\_R_2}+\frac{1}{2}\mathrm{P}_{a,r}+\frac{3}{2}\mathrm{P}_{b,r}$
$N=3$	$\frac{3}{2}\mathrm{P}_{xor\_R_1}+\mathrm{P}_{xor\_R_2}+\frac{3}{2}\mathrm{P}_{xor\_R_3}+\frac{1}{2}\mathrm{P}_{a,r}+\frac{1}{2}\mathrm{P}_{b,r}$
$N=4$	$2\mathrm{P}_{xor\_R_1}+\mathrm{P}_{xor\_R_2}+2\mathrm{P}_{xor\_R_3}+\mathrm{P}_{xor\_R_4}+\mathrm{P}_{a,r}+2\mathrm{P}_{b,r}$
$N=5$	$2\mathrm{P}_{xor\_R_1}+\mathrm{P}_{xor\_R_2}+2\mathrm{P}_{xor\_R_3}+\mathrm{P}_{xor\_R_4}+2\mathrm{P}_{xor\_R_5}+\mathrm{P}_{a,r}+\mathrm{P}_{b,r}$
$N=6$	$2\mathrm{P}_{xor\_R_1}+\frac{3}{2}\mathrm{P}_{xor\_R_2}+\frac{5}{2}\mathrm{P}_{xor\_R_3}+\mathrm{P}_{xor\_R_4}+\frac{5}{2}\mathrm{P}_{xor\_R_5}+\frac{3}{2}\mathrm{P}_{xor\_R_6}+\frac{1}{2}\mathrm{P}_{a,r}+2\mathrm{P}_{b,r}$
$N=7$	$2\mathrm{P}_{xor\_R_1}+\frac{3}{2}\mathrm{P}_{xor\_R_2}+\frac{5}{2}\mathrm{P}_{xor\_R_3}+\mathrm{P}_{xor\_R_4}+\frac{5}{2}\mathrm{P}_{xor\_R_5}+\frac{3}{2}\mathrm{P}_{xor\_R_6}+2\mathrm{P}_{xor\_R_7}+\frac{1}{2}\mathrm{P}_{a,r}+\frac{1}{2}\mathrm{P}_{b,r}$

is erroneous. However, each of them contains one erroneous estimation on Y_2. Thus, all the estimations of $Y_4, Y_6, \cdots$ are correct. In the j-th slot, where $j \in \{14, 18, \cdots\}$, the received symbol combination $X_{\frac{j}{2}} \oplus X_{\frac{j}{2}-1} \oplus Y_{\frac{j}{2}-2} \cdots Y_3 \oplus X_2 \oplus Y_1$ is correct. Each of them contains two erroneous estimations Y_3 and Y_1, which results in a correct XOR result. Thus, the estimations of $Y_5, Y_7, \cdots$ are correct. For B, in the i-th slot, $i \in \{12, 16, \cdots\}$, the received symbol combination $Y_{\frac{i}{2}} \oplus Y_{\frac{i}{2}-1} \oplus X_{\frac{i}{2}-2} \cdots X_2 \oplus Y_1$ is correct, and each of them contains the correct information only. Thus, the estimations of $X_4, X_6, \cdots$ are correct. In the j-th slot, where $j \in \{14, 18, \cdots\}$, the received symbol combination $Y_{\frac{j}{2}} \oplus Y_{\frac{j}{2}-1} \oplus X_{\frac{j}{2}-2} \cdots X_3 \oplus Y_2 \oplus X_1$ is erroneous, and each of them contains one erroneous estimation X_3 only. Thus, the estimations of $X_5, X_7, \cdots$ are correct. In summary, the estimations after the tenth slot are no longer affected by the error happens at R_1 in the fifth slot.

In general, if and only if single multi-access estimation error happens at relays R_1, R_2, R_3, R_4 and R_5, it will result in 4, 2, 4, 2 and 4 bits end-to-end estimation errors, respectively. Similarly, if and only if the single-hop transmission error from R_1 (R_5) to source A (B), it will result in two bits in error. Note that when there are more than one multi-access and single-hop errors happening, the impact of multiple errors can be partly cancelled. For example, if both of the multi-access errors happen at R_1 and R_3 in the fifth slot, it will result in 2 bits in errors, i.e., only $\hat{X}_2$ and $\hat{Y}_1$ are in error, instead of 8 bits in error. Thus, the end-to-end BER can be bounded by summing the impacted bits of single multi-access or single-hop transmission error. The end-to-end BER bound of D-MPNC with $N=5$ can be obtained by

$$\mathrm{P}_{e2e} = \frac{\sum_{i=1}^{5} w_i \mathrm{P}_{xor\_R_i} + 2\mathrm{P}_{a,r} + 2\mathrm{P}_{b,r}}{2}, \tag{16}$$

where $\mathrm{P}_{xor\_R_i}$ denotes the multiple-access error probability at relay R_i and $w_i = \{4, 2, 4, 2, 4\}$ denotes the numbers of end-to-end bit estimation errors impacted by the error propagation. Different from the traditional PNC with a single relay, in multi-hop PNC, the impact of the mutual-interference should be considered as introduced in Sec. III-D. For each receiver, SINR should be considered instead of SNR. Thus, in (16), to calculate $\mathrm{P}_{xor\_R_i}$, $\mathrm{P}_{a,r}$ and $\mathrm{P}_{b,r}$, the noise spectral density $2\sigma^2$ in (10)–(14) should be updated as

$$2\sigma^2 + \sum_{i=1}^{\lfloor \frac{k-1}{3} \rfloor} \frac{2E_b}{N+2} \left(\frac{(2i+1)d}{N+1}\right)^{-\alpha} + \sum_{j=1}^{\lfloor \frac{N+2-k}{3} \rfloor} \frac{2E_b}{N+2} \left(\frac{(2j+1)d}{N+1}\right)^{-\alpha} \tag{17}$$

from (8) by considering the interference from the other transmitting nodes.

For D-MPNC with other N, the lower bound end-to-end BER can be obtained similarly as the analysis for D-MPNC with $N=5$. The end-to-end BER bound for D-MPNC with N from 2 to 7 are summarized in Table I. Note that when N is an even number, at source B, if the received symbol from relay R_N is estimated in error, it will further impact on the correctness of the transmitted symbol from source B in the next slot. For example, for D-MPNC with $N=2$, we have

$$\mathrm{P}_{e2e} = \frac{w_1 \mathrm{P}_{xor\_R_1} + w_2 \mathrm{P}_{xor\_R_2} + \mathrm{P}_{a,r} + (1+w_2)\mathrm{P}_{b,r}}{2}, \tag{18}$$

where $w_1 = 3$ and $w_2 = 2$.

V. DESIGN OF S-MPNC

In this section, we present the design of S-MPNC, which targets on maximizing the end-to-end throughput and generalizing the design of multi-hop PNC with an arbitrary number of relays. The received information in the previous slots are properly applied at the sources and relays in S-MPNC. There is a tradeoff between the applications of D-MPNC and S-MPNC as discussed in Sec. V-D.

A. Generalization of S-MPNC

D-MPNC benefits from the simple implementation as the operations of the relays remain the same as that of the traditional PNC with a single relay. However, in D-MPNC, single multiple-access error at the relay may result in more than 2-bit end-to-end estimation errors especially when the number of relays is large. By properly applying the previously received information at the relays, we propose and generalize S-MPNC where single multiple-access error at the relay or single-hop transmission error at the source will only result in 2-bit end-to-end estimation errors, which is the best achievable BER performance.

A straightforward explanatory graph of for the generalization of S-MPNC is shown in Fig. 6. Note the final generalization of S-MPNC needs slight modification as explained later. In Fig. 6, each of the sources and the relays maintains a buffer which stores the last received binary result or the network-coded symbol obtained by (2), respectively. All the sources and the relays transmit the XOR result of the target information, i.e., the source data for the source and the network-coded symbol for the relay, and the information stored in the buffer, and then update the buffer by the newly received binary result. For example, in Fig. 6(a), in the third slot, source A transmits $X_2 \oplus X_1 \oplus Y_1$, where X_2 is the target information and

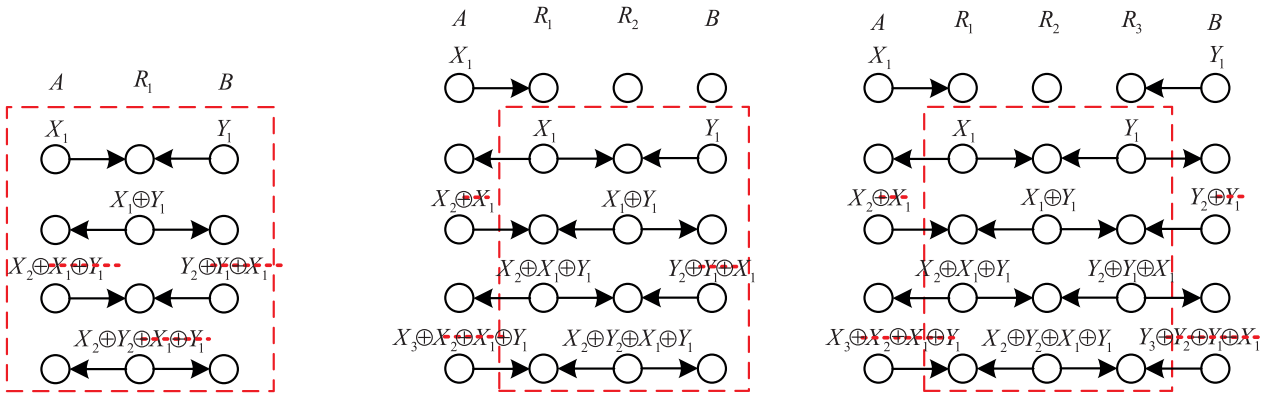

(a) S-MPNC with $N=1$. (b) S-MPNC with $N=2$. (c) S-MPNC with $N=3$.

Fig. 6. Generalization of S-MPNC.

$X_1 \oplus Y_1$ is the last received binary result in the second slot and stored in the buffer. In the fourth slot, the relay broadcasts $X_2 \oplus Y_2 \oplus X_1 \oplus Y_1$, which is the XOR result of the newly obtained network-coded symbol $X_2 \oplus X_1 \oplus Y_1 \oplus Y_2 \oplus Y_1 \oplus X_1 = X_2 \oplus Y_2$ in the last slot and the network-coded symbol $X_1 \oplus Y_1$ obtained in the first slot and stored in the buffer. Comparing Figs. 6(a), 6(b) and 6(c), we can easily observe that the kernel part marked by the red dashed square is always the same with the increase of the relay number. Thus, it can be extended and generalized for with an arbitrary relay number N.

Note that the above explanations help to identify the relations of S-MPNC with an arbitrary number of relay and prove that S-MPNC can be easily generalized. However, the final generalization of S-MPNC needs modifications for the operations of the sources and the sources' neighbouring relays in order to minimize the impact of the error propagation. Considering the symbol combinations of the relays that are not the sources' neighbours, the following two operations are equivalent:

1) Operation-1: both sources and their neighbouring relays simply transmit the target information, i.e., the same as that of the traditional PNC.

2) Operation-2: both sources and their neighbouring relays transmit the XOR result of the target information and the last binary information or received network-coded symbol, i.e., as that shown in Fig. 6 without erasing the bits marked by the red dashed lines.

Note that Operation-1 and Operation-2 refers to erase or without erase the bits marked by the red dashed lines in Fig. 6. Operation-2 is the straightforward explanation introduced above and Operation-1 will lead to the final generalization of S-MPNC.

We give an example to compare these two operations. In Fig. 6(c), erasing the bits marked by the red dashed lines, i.e., Operation-1, and remaining these bits, i.e., Operation-2, have the same impact to the symbol combination at the 2-th relay. From Operation-2, we can easily observe the pattern of the S-MPNC generalization with an arbitrary number of relay. However, considering the error propagation of the single-hop transmission from the sources' neighbouring relays to the sources, Operation-1 outperforms Operation-2 in terms of end-to-end BER. Thus, an equivalent transformation from Operation-2 to Operation-1 referring to the symbol combinations at the relays is necessary for the final generalization of S-MPNC.

The generalization of S-MPNC with an odd[7] number of relay N can be summarized as follows:

1) The sources transmit X_i and Y_i in the odd slots.

2) The j-th relay, $j \in \{2, 4, \cdots, N-1\}$, transmits in the odd slots and receives in the even slots. The j-th relay, $j \in \{1, 3, \cdots, N\}$, receives in the odd slots and transmits in the even slots.

3) The operations of the sources' neighbouring relays are the same as that of the traditional PNC or D-MPNC. The other relays broadcast the XOR results of the newly received network-coded symbol and the last received network-coded symbol.[8]

The transmission graph after erasing the binary bits marked by the red dashed lines in Fig. 6 can be obtained by the above generalization. We use an example to explain the generalization of S-MPNC. By criteria 1) and 2), S-MPNC with $N=1$ deteriorates to the traditional PNC with a single relay as shown in Fig. 6(a), where the binary bits marked by the red dashed lines are erased. Criterion 3) can be explained in Fig. 6(c), where the operations of the two relays neighbouring to the sources are the same as that in the traditional PNC or D-MPNC. However, the second relay needs to broadcast the XOR result of the newly obtained network-coded symbol and the last obtained network-coded symbol.

Note that criterion 3) can be achieved by maintaining and updating a buffer at each of the relays except the sources' neighbouring relay(s). At each transmitting slot i of the relay, the buffer stores the previously obtained network-coded symbol in the $(i-3)$-th slot, and then be updated to store the newly obtained network-coded symbol in the $(i-1)$-th slot.

B. Generalizing the Iterative Decoding Algorithm of S-MPNC

Similarly to the decoding algorithm design of D-MPNC, in S-MPNC, the sources first need to identify the pattern of the received symbol combinations from the neighbouring

[7] When N is even, source B needs to transmit with one-slot delay comparing to source A as shown in Fig. 6(b).

[8] It can be achieved by maintaining a buffer at each of the relays.

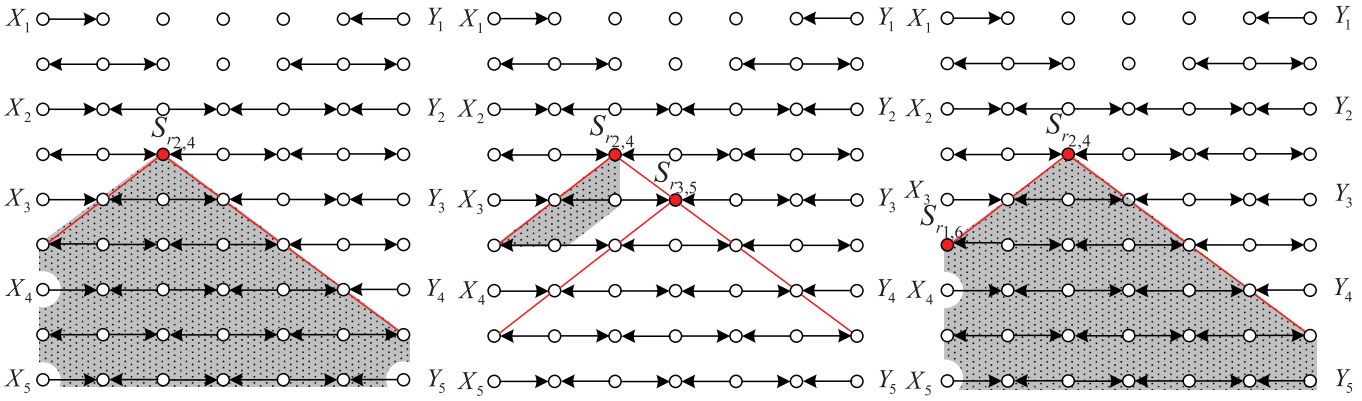

(a) Case 1. (b) Case 2. (c) Case 3.

Fig. 7. Lower bound end-to-end BER analysis of S-MPNC.

relays, and then extract the target information from the symbol combinations. We use source A as an example to introduce the decoding algorithm design and the decoding algorithm at source B is similar. In the i-th slot, where i is an even integer, $i \in \{2, 4, \cdots\}$, the received symbol combination at source A from the first relay can be expressed as

$$\hat{S}_{r_{1i}} = \hat{Y}_{\frac{i-N+1}{2}} \oplus \sum_{m=1}^{\frac{i}{2}} X_m \oplus \sum_{n=1}^{\frac{i-N-1}{2}} \hat{Y}_n, \tag{19}$$

where $\sum_{i=1}^{N} x_i = x_1 \oplus x_2 \cdots \oplus x_N$ defines the mod-2 summation and $\hat{Y}_j = 0$ if $j \leq 0$. $\hat{S}_{r_{1i}}$ is the estimated binary result from R_1 and the target estimated symbol from source B is $\hat{Y}_{\frac{i-N+1}{2}}$. Note that in (19), $\sum_{n=1}^{\frac{i-N-1}{2}} \hat{Y}_n$ denote the summation of the mod-2 addition of all the previous estimations of Y_j, $j \in \{1, \cdots, \frac{i-N-1}{2}\}$.

Source A needs to apply and update a buffer denoted as B_a in the iterative decoding algorithm. The coding algorithm of S-MPNC at source A can be summarized as follows:

1) In the i-th slot, $i \in \{N+1, N+3, \cdots\}$, obtain the symbol combination $\hat{S}_{r_{1i}}$ by (5).

2) Extract the target information $\hat{Y}_{\frac{i-N+1}{2}}$ from $\hat{S}_{r_{1i}}$ by

$$\hat{Y}_{\frac{i-N+1}{2}} = \hat{S}_{r_{1i}} \oplus B_a \oplus X_{N-1}, \tag{20}$$

where buffer B_a is initialized as $X_1 \oplus X_2 \cdots X_{N-2}$ in the $(N+1)$-th slot.

3) Update buffer $B_a = \hat{S}_{r_{1i}}$.

We use Fig. 6(c) as an example to explain the decoding algorithm of S-MPNC. In step 1), in the fourth slot, which is the first slot that source A receives the target information Y_1 from source B. Source A receives and obtains the estimation of symbol combination $\hat{S}_{r_{1,i}}$ by (5), which can be expressed as $\hat{S}_{r_{1,i}} = X_2 \oplus X_1 \oplus \hat{Y}_1$ by (19). In step 2), source A can extract the target information $\hat{Y}_1 = \hat{S}_{r_{1,i}} \oplus B_a \oplus X_2$, where buffer B_a is initialized as X_1. Finally, buffer B_a is updated to store the received binary result $\hat{S}_{r_{1,i}}$, which will be further applied to detect Y_2 in the sixth slot.

Note that in (19), $\sum_{m=1}^{\frac{i}{2}} X_m$ is always correct as it is known by source A. $\hat{S}_{r_{1,i}}$ is the estimation of the received symbol combination from R_1 and $\sum_{n=1}^{\frac{i-N-1}{2}} \hat{Y}_n$ is the summation of all the previous estimations of Y_j, $j \in \{1, \cdots, \frac{i-N-1}{2}\}$. Thus, both of them may be erroneous. However, in the next subsection we will show that the error prorogation of the single multiple-access error at the relays or the single-hop transmission from R_1 (R_N) to source A (B) will be 2-bit end-to-end estimation errors. If more than one multiple-access and single-hop errors happen, the end-to-end BER of S-MPNC will be bounded by considering the summation of the individual impact of each error events explained in the following subsection.

C. End-to-End BER Analysis of S-MPNC

S-MPNC can achieve the end-to-end BER bound expressed as

$$\sum_{i=1}^{N} \mathrm{P}_{xor\_R_i} + \mathrm{P}_{a,r} + \mathrm{P}_{b,r}, \tag{21}$$

where $\mathrm{P}_{xor\_R_i}$ is the error rate of the multiple-access transmission at the i-th relay, $i \in \{1, 2, \cdots, N\}$, and $\mathrm{P}_{a,r}$ and $\mathrm{P}_{b,r}$ are the single-hop transmission error rate from relay R_1 (R_N) to source A (B).

1) Impact of the Error Propagation: We first consider the single multiple-access error at any of the relays. For the j-th relay, in the i-th slot, if and only if the obtained network-coded symbol $\hat{S}_{r_{j,i}}$ is in error, it will result in 2-bit estimation error at each source, i.e., the estimations of $\hat{Y}_{\frac{i+j-N+1}{2}}$ and $\hat{X}_{\frac{i-j}{2}}$ are erroneous.

Proof: If and only if $\hat{S}_{r_{j,i}}$ is in error, the errors will propagate to the neighbour nodes in the following slots as shown in Fig. 7(a). The received or transmitted symbols of the nodes in the shadow region will be erroneous.[9] The binary estimation error starts from $S_{r_{j,i}}$ and propagates to R_1 and R_N in j slots and $(N-j)$ slots, respectively. The first erroneous symbol combination at source A from R_1 is

$$\hat{S}_{r_{1,i+j}} = \hat{Y}_{\frac{i+j-N+1}{2}} \oplus \sum_{m=1}^{\frac{i+j}{2}} X_m \oplus \sum_{n=1}^{\frac{i+j-N-1}{2}} \hat{Y}_n, \tag{22}$$

[9]The information transmitted from the sources are always correct in S-MPNC as no previously received information is applied in the transmitting signals.

where $\hat{S}_{r_{1,i+j}}$ is erroneous and $\sum_{m=1}^{\frac{i+j}{2}} X_m \oplus \sum_{n=1}^{\frac{i+j-N-1}{2}} \hat{Y}_n$ is correct. Thus, end-to-end estimation $\hat{Y}_{\frac{i+j-N+1}{2}}$ is erroneous. Similarly, end-to-end estimation $\hat{X}_{\frac{i-j}{2}}$ is erroneous at source B.

However, we will show that all other end-to-end estimations after $\hat{Y}_{\frac{i+j-N+1}{2}}$ and $\hat{X}_{\frac{i-j}{2}}$ are correct. The estimation of $\hat{Y}_{\frac{i+j-N+3}{2}}$ can be obtained by

$$\hat{S}_{r_{1,i+j+2}} = \hat{Y}_{\frac{i+j-N+3}{2}} \oplus \sum_{m=1}^{\frac{i+j+2}{2}} X_m \oplus \sum_{n=1}^{\frac{i+j-N+1}{2}} \hat{Y}_n, \quad (23)$$

where $\hat{S}_{r_{1,i+j+2}}$ and $\sum_{n=1}^{\frac{i+j-N+1}{2}} \hat{Y}_n$ are erroneous and $\sum_{m=1}^{\frac{i+j+2}{2}} X_m$ is correct. Thus, end-to-end estimation $\hat{Y}_{\frac{i+j-N+3}{2}}$ is correct. For any $\hat{Y}_k$, $k > \frac{i+j-N+1}{2}$, as in (23), the term on the left-side of '=' and the third term on the right-side of '=' are always erroneous, and the second term on the right-side of '=' is correct. Thus, the target information in first term on the right-side of '=' is correct. We can similarly obtain that all $\hat{X}_k$, $k > \frac{i-j}{2}$ are correct. Thus, single multiple-access error at any relay will result in 2-bit end-to-end estimation errors.

Second, we study the impact of the individual single-hop transmission error from relay R_1 (R_N) to source A (B). If and only if an error happens over the hop from R_1 (R_N) to source A (B), which will result in 2-bit end-to-end estimation errors at source A (B).

Proof: At the i-th slot, $i \in \{N+1, N+3, \cdots\}$, the received symbol combination at source A from the first relay is

$$\hat{S}_{r_{1,i}} = \hat{Y}_{\frac{i-N+1}{2}} \oplus \sum_{m=1}^{\frac{i}{2}} X_m \oplus \sum_{n=1}^{\frac{i-N-1}{2}} \hat{Y}_n. \quad (24)$$

The target information $\hat{Y}_{\frac{i-N+1}{2}}$ is erroneous as the estimation of symbol combination $\hat{S}_{r_{1,i}}$ is erroneous. In the $(i+2)$-th slot, $i \in \{N+3, N+5, \cdots\}$, the received symbol combination is

$$\hat{S}_{r_{1,i+2}} = \hat{Y}_{\frac{i-N+3}{2}} \oplus \sum_{m=1}^{\frac{i+2}{2}} X_m \oplus \sum_{n=1}^{\frac{i-N+1}{2}} \hat{Y}_n. \quad (25)$$

The target information $\hat{Y}_{\frac{i-N+3}{2}}$ is erroneous as the estimation of symbol combination $\hat{S}_{r_{1,i+2}}$ is correct, but $\sum_{n=1}^{\frac{i-N+1}{2}} \hat{Y}_n$ is erroneous due to the erroneous $\hat{Y}_{\frac{i-N+1}{2}}$. However, it is easy to see that any $\hat{Y}_k$, $k > \frac{i-N+3}{2}$ is correct as the errors in $\hat{Y}_{\frac{i-N+3}{2}}$ and $\hat{Y}_{\frac{i-N+1}{2}}$ cancel. Thus, the single-hop transmission error will result in 2-bit end-to-end estimation errors.

Third, we study the cases when there are more than one multiple-access and single-hop transmission errors. When more than one multiple-access and single-hop errors happen, the total end-to-end estimation errors are smaller than that of summing each of the error event individually, as the fact that the impact of multiple errors may cancel each other. We provide two examples as shown in Figs. 7(b) and 7(c) to explain. In Fig. 7(b), the error regions caused by erroneous estimations $\hat{S}_{r_{2,4}}$ and $\hat{S}_{r_{3,5}}$ are cancelled, which will result in 2-bit estimation errors, i.e., $\hat{Y}_1$ and $\hat{Y}_2$, instead of 4-bit end-to-end estimation errors. Erroneous $\hat{Y}_2$ is caused by the impact of the erroneous estimation $\hat{Y}_1$. In Fig. 7(c), if two multiple-access transmission $\hat{S}_{r_{2,4}}$ and single-hop transmission $\hat{S}_{r_{1,6}}$ are erroneous, which will result in 1-bit end-to-end estimation, i.e., $\hat{X}_2$ is erroneous, instead of 4-bit end-to-end estimation errors. Thus, When more than one multiple-access and single-hop errors happening, the total end-to-end estimation errors are smaller than that of summing the bit errors caused by each of the error event individually. Thus, an end-to-end BER bound in (21) can be achieved by S-MPNC.

2) Impact of the Interference From Other Transmitting Nodes: In multi-hop PNC, for each receiver, the mutual-interference from other transmitting nodes besides the neighbouring nodes should be considered. To calculate $P_{xor\_R_i}$, $P_{a,r}$ and $P_{b,r}$ in (21), the noise spectral density $2\sigma^2$ in (10)–(14) should be updated as (17). Note that the impact of the interference and that of the error propagation in multi-hop PNC are independent. The impact of the error propagation are caused by the properties of the network-coded and multi-hop topology, which can be optimized by properly applying the previous information and design the symbol combination pattern. The impact of the interference are caused by the physical channels, which can be optimized by enlarging the hop-distance of the interference nodes. However, the end-to-end throughput will also be negatively affected by enlarging the hop-distance of the interference nodes due to the overall transmission efficiency.

D. Comparison Between D-MPNC and S-MPNC

In this paper, we propose two designs with different design purposes. D-MPNC benefits from the simple-implementation, as the operations of all the relays are exactly the same as that of the traditional PNC with a single relay. Also the sources simply transmit the target symbol when the number of the relays is odd, the same as that of the traditional PNC with a single relay. The key issue is the detection of the target symbol from the other sources in the obtained symbol combination as elaborated in Sec. IV-B. Thus, in D-MPNC, all the relays remain the same and simple operations. To upgrade from the traditional PNC with a single relay to D-MPNC, only the detection algorithm at the sources are required to be upgraded, which can be easily achieved by software upgradation. S-MPNC targets for the optimal end-to-end BER performance by taking advantage of the fact that the previously obtained information at any node can be positively applied. The relays except the sources' neighbours are equipped with one buffer to store the previously obtained information and updated these information in every two slots. In other words, the sources' neighbouring relays and the other relays have different operations as discussed in Sec. V-A. In the initializing stage, the sources need signalling to inform the relays whether they are or not the sources' neighbouring. The end-to-end BER bounds of D-MPNC and S-MPNC are summarized in Table I and (21), respectively, and further compared in Sec. VI-A. From the end-to-end BER perspective, S-MPNC outperforms D-MPNC benefiting from the better error propagation control. To summary, there is a tradeoff between D-MPNC and S-MPNC depending on the implementation complexity and throughput gain perspectives.

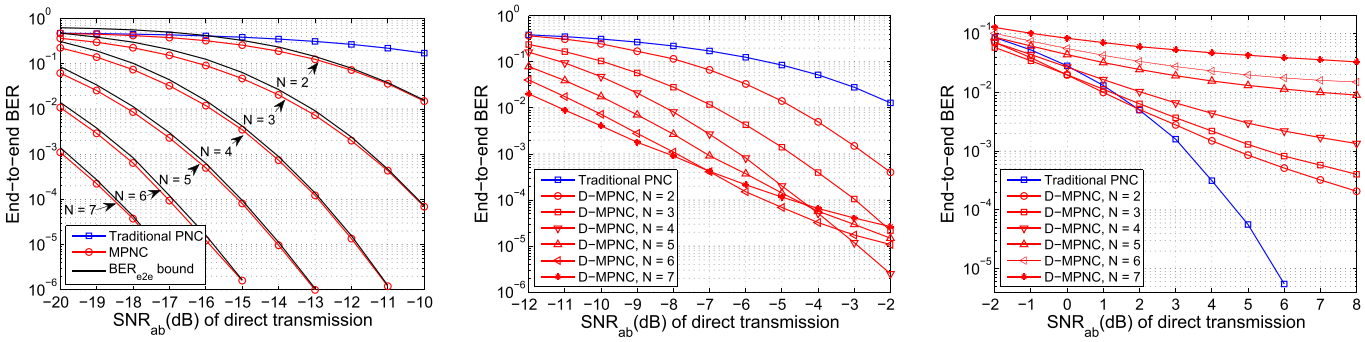

(a) $\alpha = 4$. (b) $\alpha = 3$. (c) $\alpha = 2$.

Fig. 8. End-to-end BER performance of D-MPNC under AWGN channel.

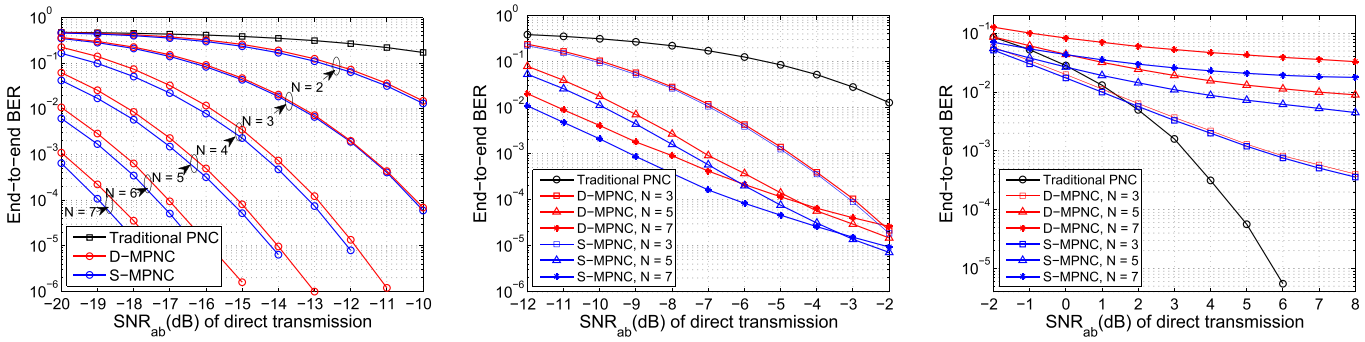

(a) $\alpha = 4$. (b) $\alpha = 3$. (c) $\alpha = 2$.

Fig. 9. End-to-end BER performance of S-MPNC under AWGN channel.

VI. Performance Evaluation

In this section, the performance of the proposed multi-hop PNC schemes are evaluated. For any PNC scheme, we let the total transmission power in any two continuous slots be $2E_b$, and all the nodes equally share the total transmission power. The nodes are located in a linear topology. The average received SNR of all links are proportional to $d^{-\alpha}$, where d is the transmission distance and α is the path-loss exponent. We studied the performance of D-MPNC and S-MPNC under both AWGN and Rician channels with various parameter settings, and the impact of the relays' locations in multi-hop PNC are further studied.

A. Performance of End-to-End BER Under AWGN Channel

The end-to-end BER performance of D-MPNC and S-MPNC under AWGN channel are shown in Figs. 8 and 9. In the figures, the X axis is the end-to-end SNR$_{ab}$ (dB) by direct transmission without PNC in (6). Given SNR$_{ab}$ (dB), the distance between sources A and B, d, is the same and fixed for all different transmission schemes applied. For the traditional PNC or multi-hop PNC with N relay(s), the transmission power for each node is $\frac{2E_b}{N+2}$ and the transmission distance of each hop is $\frac{d}{N+1}$. Thus, there is a tradeoff between the transmission power and hop-distance by difference number of relay N. The path-loss exponent α, which is normally set to be from 2 to 6 [28], has two impact on the performance of multi-hop PNC. Given the end-to-end SNR$_{ab}$ (dB) in (6) and the distance d (m) between the sources, the larger α is, the SINR (dB) of each hop in (8) is larger by shortening the transmission path. Another impact is that a larger α reduces the impact of the mutual-interference from other transmitting nodes to the receiver due to a larger path loss. The impact of the path-loss exponent α are studied in this section.

The end-to-end BER performance of D-MPNC is shown in Fig. 8 with different path-loss exponent α. In Fig. 8(a), the black curves are the end-to-end BER bound of D-MPNC obtained in Table I and the red circle curves are the exact end-to-end BER performance. We can see that when the BER is lower, the bound approaches the exact end-to-end BER, because when BER is lower, the probability that more than one multiple-access and single-hop errors happen in the same slot becomes smaller, and individual multiple-access error or single-hop error dominates the end-to-end error performance. Comparing Figs. 8(a), 8(b) and 8(c), we can see that the path-loss exponent α impacts on the end-to-end BER performance. In Fig. 8(a), D-MPNC outperforms the traditional PNC with a single relay significantly due to a relatively larger SINR between the neighbouring nodes and a relatively smaller interference impact from other transmitting nodes. In Fig. 8(c), the traditional PNC with a single relay outperforms D-MPNC, as a relatively larger mutual-interference from other transmitting nodes to the receivers and a relatively smaller gain from shortening the transmission distance. In Figs. 8(b) and 8(c), with the increase of end-to-end SNR$_{ab}$ (dB), the end-to-end BER performance converge with a larger relay number N. Because the mutual-interference

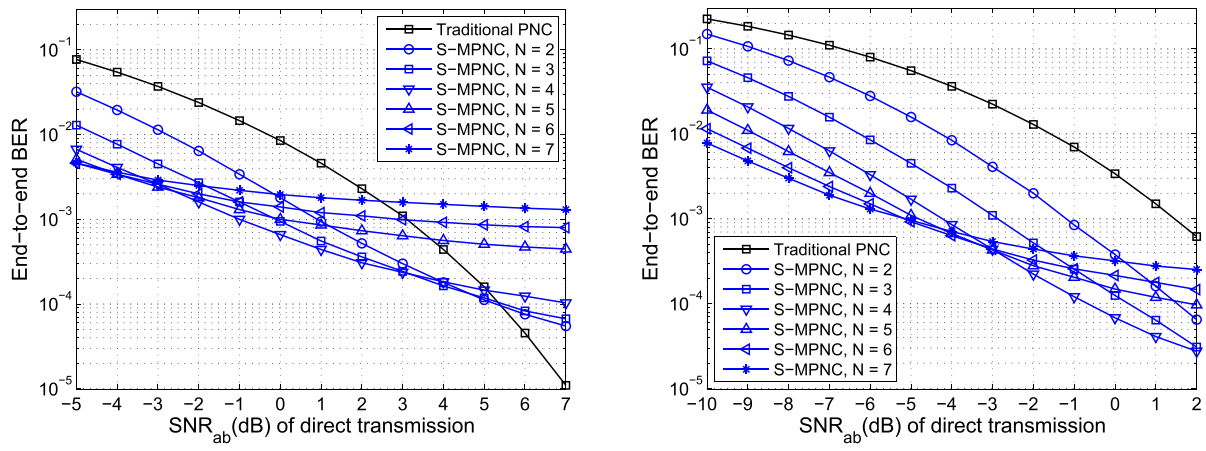

(a) $K_{rician} = 0.2$. (b) $K_{rician} = 0.4$.

Fig. 10. End-to-end BER performance of S-MPNC under Rician channel with path-loss exponent $\alpha = 3$.

from other transmitting nodes in multi-hop PNC also increases with the increase of SNR$_{ab}$ (dB), and the SINRs of two neighbouring nodes approach to the upper bound. Further increasing SNR$_{ab}$ (dB) will not help to improve the end-to-end BER, as the SNR of each hop is upper bounded by $10\alpha \log_{10} 3$ (dB) as explained in Sec. III-D.

Fig. 9 compares the end-to-end BER performance of D-MPNC and S-MPNC with different α. S-MPNC outperforms D-MPNC in terms of end-to-end BER, as S-MPNC further reduces the error propagation effects by enabling the relays to properly applying the previously received information. Note that the receiver in S-MPNC is also impacted by the interference from other transmitting nodes, which is independent to the impact of the error propagation. However, S-MPNC always outperforms D-MPNC in terms of end-to-end BER under arbitrary channels due to a smaller error propagation effect. From Figs. 8 and 9 and (8), we can see that both the error propagation and mutual-interference determine the throughput gain of multi-hop PNC. When the path-loss exponent α is large, the mutual-interference is relatively small. Thus, with the increase of the number of relays, the per-hop SINR is enlarged thanks to the shortened hop distance, and the error propagation impact is well controlled. However, when α is small, with the increase of the number of relays, the mutual-interference may dominate the per-hop SINR. In this case, the throughput with a smaller number of relays may be higher. Generally speaking, multi-hop PNC designs are more suitable for the scenarios with poor channel conditions between the sources and/or low transmission power used in the system.

Fig. 9 identifies the end-to-end BER performance gap between D-MPNC and S-MPNC, in the following section, we only present the performance of S-MPNC, and the performance of D-MPNC can be easily inferred.

B. Performance of End-to-End BER Under Rician Channel

In the subsection, we study the end-to-end BER performance of S-MPNC under Rician channel as shown in Figs. 10 and 11 with different path-loss exponent α and Rician parameter K_{rician}. K_{rician} is the ratio between the power in the direct path and the power in other scattered paths. Fig. 10 shows the end-to-end BER performance of S-MPNC with $\alpha = 3$. In Fig. 10(a), when the end-to-end SNR$_{ab}$ is low, e.g., from -5 dB to 2 dB, S-MPNC outperforms the traditional PNC with a single relay. However, the traditional PNC outperforms S-MPNC by further increasing SNR$_{ab}$ (dB) as the increase of the interference from other transmitting node. Comparing Figs. 10(a) and 10(b), we can see that a larger end-to-end SNR$_{ab}$ (dB) is required to maintain the same BER level with a larger K_{rician}.

Fig. 11 shows the end-to-end BER performance of S-MPNC with $\alpha = 4$. We can see that with a larger $\alpha = 4$, S-MPNC outperforms the traditional PNC significantly. In Fig. 11(a), for S-MPNC with $N = 7$, the end-to-end BER begins to converge at about -8 dB, which implies the end-to-end BER performance will not improve by further increasing the number of relays.

C. Impact of the Relays' Locations

In this subsection, the throughput performance of S-MPNC and the impact of the relays' locations are studied. We let each block contains 256 bits, if any bit in the block is estimated in error, the block is dropped without retransmission. The throughput (bits/slot) is defined as the successfully received bits per slot by all the destinations. The blue and black dotted curves in Figs. 12 and 13 show the throughput performance of S-MPNC and the traditional PNC with different path-loss parameter settings, where the relays are evenly located in a linear topology between the sources. From Figs. 12 and 13, generally speaking, S-MPNC outperforms the traditional PNC with a single relay in the lower end-to-end SNR$_{ab}$ (dB) region, and the larger the path-loss exponent and the smaller the Rician parameter K_{rician} is, the more throughput gain S-MPNC can achieve compared to the traditional PNC.

We also studied the impact of the relays' locations on the throughput performance of S-MPNC. For S-MPNC with N relays, we let the location of the j-th relay, $j \in \{1, 2, \cdots, N\}$, follows a uniform distribution with the mean

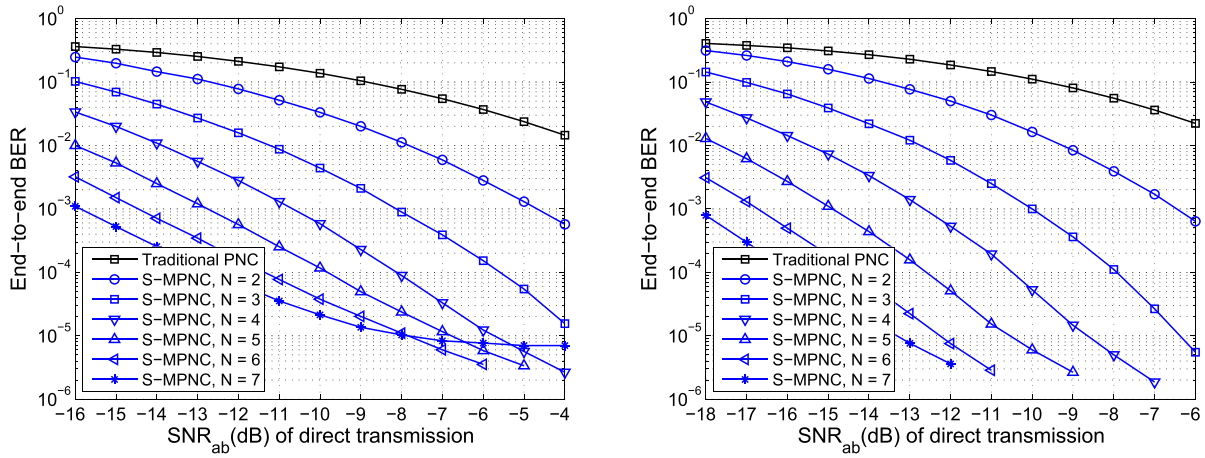

(a) $K_{rician} = 0.2$. (b) $K_{rician} = 0.4$.

Fig. 11. End-to-end BER performance of S-MPNC under Rician channel with path-loss exponent $\alpha = 4$.

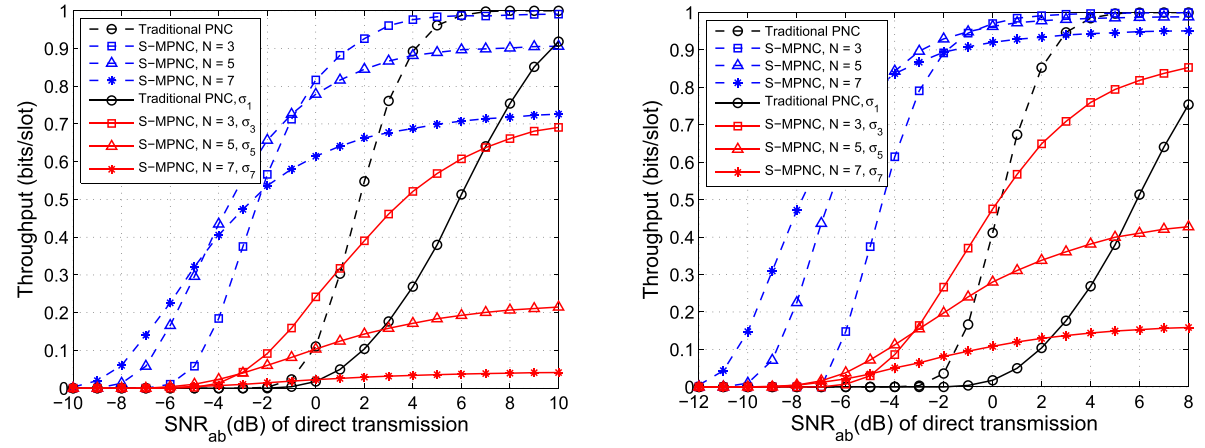

(a) $K_{rician} = 0.2$. (b) $K_{rician} = 0.4$.

Fig. 12. Impact of non-perfect relay locations with path-loss exponent $\alpha = 3$.

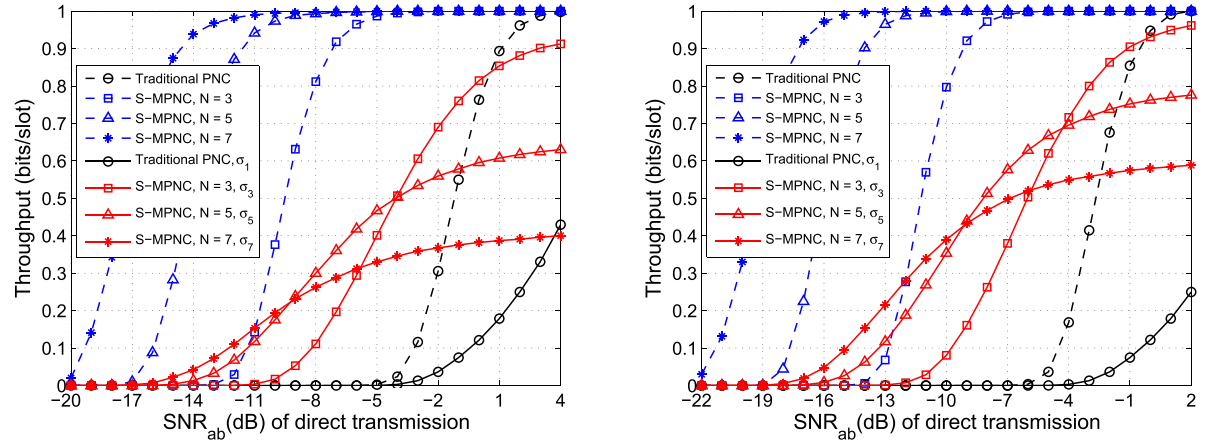

(a) $K_{rician} = 0.2$. (b) $K_{rician} = 0.4$.

Fig. 13. Impact of non-perfect relay locations with path-loss exponent $\alpha = 4$.

$\frac{d}{N+1}$ and the standard variance $\sigma_N = \frac{(\frac{d}{N+1})}{\sqrt{12}}$. Note that $\sigma_N = \frac{(\frac{d}{N+1})}{\sqrt{12}}$ is the largest standard variance to guarantee that two neighbouring relays will not overlap. Thus, the red solid curves in Figs. 12 and 13 show the lower bound of the throughput performance of S-MPNC with different maximal standard variance σ_i, $i \in \{1, 3, 5, 7\}$. We can see that the relays' locations in multi-hop PNC also affect the throughput

performance due to the impact of the mutual-interference. The worst case is that the locations of three neighbouring nodes, labelled as node-1, node-2 and node-3, may be too close. In this case when the left-side node of node-1, labelled as node-0, is the receiver, the interference from node-3 to node-0 would be larger enough to impact the useful signals from the node-1. The hop between node-0 and node-1 will be the bottleneck of the multi-hop transmission, which domains the end-to-end throughput performance of multi-hop PNC.

VII. Conclusion

In this paper, the design of multi-hop PNC has been investigated. We first introduced two key issues in multi-hop PNC design, including the error propagation effects and the impact of the mutual-interference from other transmitting nodes. By carefully addressing these two issues, we proposed two multi-hop PNC designs, including D-MPNC and S-MPNC, where the maximum end-to-end throughput of one symbol per symbol duration can be achieved by both designs. There is a tradeoff between the applications of D-MPNC and S-MPNC. D-MPNC benefits from the simple-implementation, as the operations of the relays remain the same as that of the traditional PNC with a single relay. S-MPNC targets to generalize the multi-hop PNC design by arbitrary number of relay with optimal end-to-end BER. S-MPNC outperforms D-MPNC in terms of end-to-end BER by enabling the relays to properly apply the previously received information. Given the end-to-end SNR, the SINR (dB) of any two neighbouring nodes is upper bounded by $10\alpha \log_{10} 3$ due to the impact of the interference from other transmitting nodes, where the value 3 is from ratio of the distance from the closest interference node to that from the transmitter to the receiver. Extensive simulation results have demonstrated that the proposed multi-hop PNC designs outperform the traditional PNC with a single relay in terms of end-to-end BER and throughput when the source nodes are far away.

One important further research issue is to design multi-hop PNC with higher-order modulation. The scheduling and iterative algorithm designs in this work can be easily extended to higher-order QAM modulation designs. For example, we can virtually split the higher-order modulation transmission into several parallel BPSK transmissions. However, higher order modulation PNC needs to deal with the singular fade states (SFS) issue, which denotes that in some specific source-relay channels, there may exist different constellation points superimposed completely on the received constellation map at the relay. Thus, how to design multi-hop PNC with higher-order modulation with well controlled SFS impact is an open issue worth further research.

References

[1] S. Zhang, S. C. Liew, and P. P. Lam, "Hot topic: Physical-layer network coding," in *Proc. ACM MobiCom*, 2006, pp. 358–365.

[2] P. Popovski and H. Yomo, "The anti-packets can increase the achievable throughput of a wireless multi-hop network," in *Proc. IEEE ICC*, Jun. 2006, pp. 3885–3890.

[3] P. Popovski and H. Yomo, "Bi-directional amplification of throughput in a wireless multi-hop network," in *Proc. IEEE VTC*, May 2006, pp. 588–593.

[4] G. Wang, W. Xiang, J. Yuan, and T. Huang, "Outage analysis of non-regenerative analog network coding for two-way multi-hop networks," *IEEE Commun. Lett.*, vol. 15, no. 6, pp. 662–664, Jun. 2011.

[5] G. Wang, W. Xiang, and J. Yuan, "Multihop compute-and-forward for generalised two-way relay channels," *Emerg. Telecommun. Technol.*, vol. 26, no. 3, pp. 448–460, 2015.

[6] G. Wang, W. Xiang, and J. Yuan, "Generalized wireless network coding schemes for multihop two-way relay channels," *IEEE Trans. Wireless Commun.*, vol. 13, no. 9, pp. 5132–5147, Sep. 2014.

[7] F. Wang, L. Guo, S. Wang, Q. Song, and A. Jamalipour, "Approaching single-hop performance in multihop networks: End-to-end known-interference cancelation (E2E-KIC)," *IEEE Trans. Veh. Technol.*, vol. 65, no. 9, pp. 7606–7620, Sep. 2016.

[8] F. Wang, L. Guo, S. Wang, Y. Yu, Q. Song, and A. Jamalipour, "Almost as good as single-hop full-duplex: Bidirectional end-to-end known interference cancellation," in *Proc. IEEE ICC*, Jun. 2015, pp. 1932–1937.

[9] S. Zhang and S.-C. Liew, "Channel coding and decoding in a relay system operated with physical-layer network coding," *IEEE J. Sel. Areas Commun.*, vol. 27, no. 5, pp. 788–796, Jun. 2009.

[10] B. Nazer and M. Gastpar, "Reliable physical layer network coding," *Proc. IEEE*, vol. 99, no. 3, pp. 438–460, Mar. 2011.

[11] S. Zhang, S.-C. Liew, and P. P. Lam, "On the synchronization of physical-layer network coding," in *Proc. IEEE Inf. Theory Workshop*, Oct. 2006, pp. 404–408.

[12] L. Lu and S. C. Liew, "Asynchronous physical-layer network coding," *IEEE Trans. Wireless Commun.*, vol. 11, no. 2, pp. 819–831, Feb. 2012.

[13] T. Koike-Akino, P. Popovski, and V. Tarokh, "Optimized constellations for two-way wireless relaying with physical network coding," *IEEE J. Sel. Areas Commun.*, vol. 27, no. 5, pp. 773–787, Jun. 2009.

[14] S. C. Liew, S. Zhang, and L. Lu, "Physical-layer network coding: Tutorial, survey, and beyond," *Phys. Commun.*, vol. 6, pp. 4–42, Mar. 2013.

[15] H. Zhang, L. Zheng, and L. Cai, "Design and analysis of heterogeneous physical layer network coding," *IEEE Trans. Wireless Commun.*, vol. 15, no. 4, pp. 2484–2497, Apr. 2016.

[16] H. Zhang, L. Zheng, and L. Cai, "PiPNC: Piggybacking physical layer network coding for multihop wireless networks," in *Proc. ICC*, Jun. 2015, pp. 6211–6216.

[17] L. Lu, T. Wang, S. C. Liew, and S. Zhang, "Implementation of physical-layer network coding," *Phys. Commun.*, vol. 6, pp. 74–87, Mar. 2013.

[18] Z. Ning, Q. Song, and Y. Yu, "A novel scheduling algorithm for physical-layer network coding under Markov model in wireless multi-hop network," *Comput. Electr. Eng.*, vol. 39, no. 6, pp. 1625–1636, 2013.

[19] J. He and S. C. Liew, "Building blocks of physical-layer network coding," *IEEE Trans. Wireless Commun.*, vol. 14, no. 5, pp. 2711–2728, May 2015.

[20] S. Lin, L. Fu, J. Xie, and X. Wang, "Hybrid network coding for unbalanced slotted ALOHA relay networks," *IEEE Trans. Wireless Commun.*, vol. 15, no. 1, pp. 298–313, Jan. 2016.

[21] S. Lin and L. Fu, "Unsaturated throughput analysis of physical-layer network coding based on IEEE 802.11 distributed coordination function," *IEEE Trans. Wireless Commun.*, vol. 12, no. 11, pp. 5544–5556, Nov. 2013.

[22] S. Lin and L. Fu, "Throughput capacity of IEEE 802.11 many-to/from-one bidirectional networks with physical-layer network coding," *IEEE Trans. Wireless Commun.*, vol. 15, no. 1, pp. 217–231, Jan. 2016.

[23] Y. Huang, S. Wang, Q. Song, L. Guo, and A. Jamalipour, "Synchronous physical-layer network coding: A feasibility study," *IEEE Trans. Wireless Commun.*, vol. 12, no. 8, pp. 4048–4057, Aug. 2013.

[24] J. Qiao, L. X. Cai, X. S. Shen, and J. W. Mark, "Enabling multi-hop concurrent transmissions in 60 Ghz wireless personal area networks," *IEEE Trans. Wireless Commun.*, vol. 10, no. 11, pp. 3824–3833, Nov. 2011.

[25] L. X. Cai, L. Cai, X. Shen, J. W. Mark, and Q. Zhang, "Mac protocol design and optimization for multi-hop ultra-wideband networks," *IEEE Trans. Wireless Commun.*, vol. 8, no. 8, pp. 4056–4065, Aug. 2009.

[26] M. Park, I. Choi, and I. Lee, "Exact BER analysis of physical layer network coding for two-way relay channels," in *Proc. IEEE VTC Spring*, May 2011, pp. 1–5.

[27] J. W. Craig, "A new, simple and exact result for calculating the probability of error for two-dimensional signal constellations," in *Proc. IEEE MILCOM*, Nov. 1991, pp. 571–575.

[28] A. Goldsmith, *Wireless Communications*. Cambridge, U.K.: Cambridge Univ. Press, 2005.

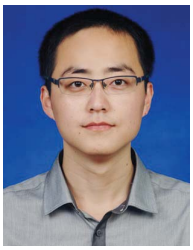

Haoyuan Zhang (S'14) received the B.S. and M.S. degrees from the Department of Electrical and Information Engineering, Harbin Institute of Technology, Harbin, China, in 2010 and 2012, respectively, and the Ph.D. degree from the Department of Electrical and Computer Engineering, University of Victoria, Victoria, BC, Canada, in 2017. His current research interests include channel error control coding, modulation optimizations, physical-layer network coding, and massive MIMO communications.

Lin Cai (S'00–M'06–SM'10) received the M.A.Sc. and Ph.D. degrees in electrical and computer engineering from the University of Waterloo, Waterloo, ON, Canada, in 2002 and 2005, respectively. Since 2005, she has been with the Department of Electrical and Computer Engineering, University of Victoria, and she is currently a Professor. Her research interests span several areas in communications and networking, with a focus on network protocol and architecture design supporting emerging multimedia traffic over wireless, mobile, ad hoc, and sensor networks. She was a recipient of the NSERC Discovery Accelerator Supplement Grants in 2010 and 2015, respectively, and the Best Paper Awards at the IEEE ICC 2008 and the IEEE WCNC 2011. She has served as TPC Symposium Co-Chair at the Globecom 2010 and Globecom 2013, an Associate Editor of the IEEE TRANSACTIONS ON WIRELESS COMMUNICATIONS, the IEEE TRANSACTIONS ON VEHICULAR TECHNOLOGY, *EURASIP Journal on Wireless Communications and Networking*, *International Journal of Sensor Networks*, and the *Journal of Communications and Networks*, and a Distinguished Lecturer of the IEEE VTS Society.